Eur. Phys. J. C 24, 447–458 (2002)
Digital Object Identifier (DOI) 10.1007/s10052-002-0955-5

THE EUROPEAN PHYSICAL JOURNAL C

Multi-jet production in hadron collisions

P.D. Draggiotis[1,2,a], R.H.P. Kleiss[1,b], C.G. Papadopoulos[2,c]

[1] University of Nijmegen, Nijmegen, The Netherlands
[2] Institute of Nuclear Physics, NCSR *Δημόκριτος*, 15310 Athens, Greece

Received: 21 February 2002 /
Published online: 22 May 2002 –

Abstract. The advent of high-energy hadron colliders necessitates efficient and accurate computation of multi-jet production processes, both as QCD processes in their own right and as backgrounds for other physics. The algorithm that performs these tasks and a brief numerical study of multi-jet processes are presented.

1 Introduction

With the recommissioning of the Tevatron, and the foreseeable commencement of physics at the LHC, the need for fast and accurate QCD calculations is now larger than ever. In this paper, we describe our efforts to arrive at results of such calculations. To set the stage: we have in mind the computation of QCD cross sections with many observed jets that, as usual, are modelled by assuming that each jet comes from a single fragmenting parton. With the large amount of energy available, the number n of jets can easily be as large as eight, thus requiring the computation of amplitudes with 10 or even more external legs.

Although in principle straightforward enough, the usual techniques of evaluating Feynman diagrams and integrating the resulting cross section by Monte Carlo are in practice hampered by the computational complexity of the problem. The following obstacles can be recognized.

(1) The flavors of the initial partons are never detected, and in most cases (barring, say, b tagging) neither are the flavors of the final-state partons. In what follows we take all quarks (u, d, s, c, and b) to be essentially massless, although a version of the code with massive fermions exists. In the case of flavor integration, to be discussed later on, we always treat quarks as massless. This means that in any given jet configuration there are usually very many contributing processes. Even enumerating these is a non-trivial task, and calculating each individual process cross section is even more so [16].
(2) In addition to flavor, neither the color nor the spin of any parton is observed. For an amplitude with p quark partons and q gluons this implies that in principle $(6)^p$ $(16)^q$ contributions have to be added. It is true that, in particular, many color configurations lead to zero amplitudes, but figuring out precisely which these are is very hard.
(3) Each individual amplitude, with specified flavors, colors and spins, contains very many Feynman diagrams. In Appendix B we give a recipe for determining the precise number of graphs, at the tree level [17]. Typical results are that the process $gg \to 8g$ is described by 10,525,900 diagrams, and the process $gg \to 2g3u3\bar{u}$ by 946,050 diagrams. Inclusion of loop corrections worsens this dramatically, of course.
(4) Each amplitude peaks in complicated ways inside the momentum phase space. Straightforward integration is therefore impractical, and one has to search for efficient mappings to do importance sampling in a multi-particle phase space.

All these difficulties are addressed in this paper, and here we describe our solutions, in reverse order.

(4) The peaking structure of the amplitude is dealt with by our phase-space generating algorithm SARGE [9,11]. This algorithm is tailored to the generation of so-called antenna structures. Let $p_1, \ldots, p_n$ be the momenta of the n partons involved. The peaking behavior of the cross section for the purely gluonic process involving n gluons, $gg \to (n-2)g$ is then dominated by the following antenna structure:

$$\Big[(p_1p_2)(p_2p_3)(p_3p_4)\cdots(p_{n-1}p_n)(p_np_1)\Big]^{-1}$$

and any permutation of labels. Since processes involving quarks do not show other dominant peaking behavior than the above ones, we can cover the n-particle momentum phase space with good efficiency. More details about SARGE can be found in [12].
(3) Over the last years new algorithms, along with their implementations, for computing the tree-order scattering amplitude have been proposed [3,13,4]. These do not involve the calculation of individual diagrams, but rather

[a] petros@sci.kun.nl
[b] kleiss@sci.kun.nl
[c] Costas.Papadopoulos@cern.ch

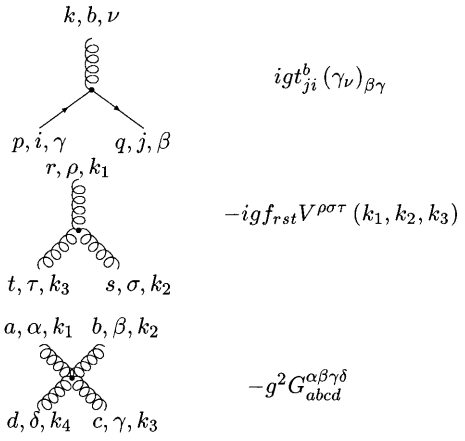

Fig. 1. Coupling of the fields in QCD

reorganize, in a systematic way, the various off-shell subamplitudes in such a way that as little of the computation as possible is repeated. The improvement in computational efficiency of these algorithms is nevertheless dramatic, down from about $n!$ to something like 3^n. In the algorithm suggested originally in [3] the scattering amplitude was computed through a set of recursive equations derived from the effective action as a function of the classical fields. These classical equations represent nothing but the tree-order Schwinger–Dyson equations, a fact that was already emphasized in subsequent approaches [4] and will be illustrated below for the special case of QCD. In fact, recursive techniques have already been used in the past to compute multi-gluon amplitudes [2].

(2) The usual spin and color summation is replaced by a Monte Carlo integration. In the purely gluonic case [13] this has been shown to work *rather* well. It must be realized that since we replace the more usual sum over discrete color and spin states by a continuous (Monte Carlo) integration, the variance of the cross section can indeed be expected to be smaller.

(1) We tackle the flavor combinatorics in the same spirit: we assign to each quark and antiquark a flavor quantum number, that is, we extend the definition of the external legs by a direct product with a flavor vector in the space of the five available flavors. By taking these vectors randomly we can perform a sum over flavors by Monte Carlo as well, and the only computational difference between the case of one single flavor and that of f flavors is simply a factor f, whereas the discrete-flavor-sum combinatorics would lead to a much bigger loss in speed. The possibility of coherent superpositions of different flavors might seem awkward but is in fact quite natural since all quarks are treated as massless and therefore the distinction between flavors is to a large extent arbitrary. The only place where flavors are *not* treated on an equal footing is in the structure functions that describe the difference in probability of picking out different flavors: by a judicious weighting of the flavor vectors for incoming quarks and antiquarks we can handle this as well.

Considering the Monte Carlo treatment of spin, color and flavor, the essential point is to realize that we are entitled to use *any* representation for the corresponding information, as long as we end up with the correct sums *on the average*.

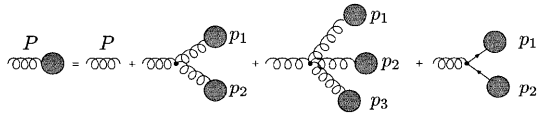

Fig. 2. Recursion equation for gluons

Before finishing this introduction we want to mention that, so far, we can calculate partonic cross sections. These are typically good for global quantities like total cross sections, p_{T} distributions and the like. A fuller treatment involves coupling the generated events to fragmentation programs like HERWIG [10]. These programs typically require additional information on the "spanning of the color string". In [7] a way to do this for processes with zero or one quark lines is described; in [18] we shall indicate how the present program can be adapted in a similar manner.

2 The algorithm for jet production

2.1 The scattering amplitude

Our starting point are the Dyson–Schwinger (DS) equations, which give recursively the n-point Green's functions. These equations hold all the information for the fields and their interactions for any number of external legs and to all orders in perturbation theory. We restrict ourselves to tree-level calculations, so we discard ghost fields. Also we consider all quarks as massless. The couplings between fields, relevant for QCD, are shown in Fig.1.

The recursive content of the DS equation, for the gluon field for example, can be understood diagrammatically as in Fig.2. The figure shows that a subamplitude with an off-shell gluon of momentum P has contributions from three- and four-vertices plus a fermion–antifermion vertex. The shaded blobs denote subamplitudes with the same structure. So, in effect, this is a recursive equation which we can write down immediately (suppressing the color):

$$
\begin{aligned}
A^\mu(P) &= \sum_{i=1}^{n} \delta_{P=p_i} A^\mu(p_i) \qquad (1)\\
&+ (\mathrm{i}g_s) \sum_{P=p_1+p_2} \Pi^\mu_\nu \bar{\psi}(p_1)\gamma^\nu \psi(p_2)\sigma(p_1,p_2)\\
&+ \frac{(\mathrm{i}g_s)}{2} \sum_{P=p_1+p_2} V^{\mu\nu\lambda}(P,p_1,p_2)A_\nu(p_1)A_\lambda(p_2)\sigma(p_1,p_2)\\
&- \frac{(g_s^2)}{6} \sum_{P=p_1+p_2+p_3} G^{\mu\nu\lambda\rho}A_\nu(p_1)A_\lambda(p_2)A_\rho(p_3)\sigma(p_1,p_2),
\end{aligned}
$$

where $V^{\mu\nu\lambda}(P,p_1,p_2)$ and $G^{\mu\nu\lambda\rho}$ are the 3- and 4-point vertices and

$$\Pi^\mu_\nu = \frac{-\mathrm{i}g^\mu_\nu}{P^2}$$

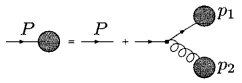

Fig. 3. Recursion equation for quarks

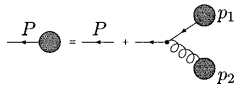

Fig. 4. Recursion equation for antiquarks

is the gluon propagator. The symbol $\sigma(p_1, p_2)$ – we will call it the sign function – takes into account the Fermi sign and has the values ± 1. More on the sign function will be presented later on. For a quark of momentum P (suppressing the color again)

$$\psi(P) = \sum_{i=1}^{n} \delta_{P=p_i} \psi(p_i) + (\mathrm{i}g_s) \sum_{P=p_1+p_2} S \not{A}(p_1)\psi(p_2)\sigma(p_1,p_2) \qquad (2)$$

(compare Fig.3), where S is the propagator

$$S = \frac{\mathrm{i}\not{P}}{P^2},$$

and for an antiquark

$$\bar{\psi}(P) = \sum_{i=1}^{n} \delta_{P=p_i} \bar{\psi}(p_i) + (\mathrm{i}g_s) \sum_{P=p_1+p_2} \bar{\psi}(p_2) \not{A}(p_1) \tilde{S} \sigma(p_1,p_2) \qquad (3)$$

(compare Fig.4), where

$$\tilde{S} = \frac{-\mathrm{i}\not{P}}{P^2}.$$

In order to reduce computational complexity, as we will discuss later on, we replace the four-gluon vertex with a three-vertex by introducing an auxiliary field $H_{\mu\nu}$. We rewrite the part of the QCD Lagrangian that describes the four-vertex in terms of the auxiliary field as follows:

$$\mathcal{L}_H = -g f^{abc} A^a_\mu A^b_\nu H^{\mu\nu c} - H^a_{\mu\nu} H^{\mu\nu a}. \qquad (4)$$

The recursion for the gluons changes slightly, namely only the part with the four-vertex. Additionally, we also have an equation for the auxiliary field (compare Fig.5):

$$\begin{aligned} A^\mu(P) &= \sum_{i=1}^{n} \delta_{P=p_i} A^\mu(p_i) \\ &+ (\mathrm{i}g_s) \sum_{P=p_1+p_2} \Pi^\mu_\nu \bar{\psi}(p_1)\gamma^\nu \psi(p_2)\sigma(p_1,p_2) \\ &+ \frac{(\mathrm{i}g_s)}{2} \sum_{P=p_1+p_2} V^{\mu\nu\lambda}(P,p_1,p_2) A_\nu(p_1) A_\lambda(p_2)\sigma(p_1,p_2) \\ &- (g_s) \sum_{P=p_1+p_2} X^{\mu\nu\lambda\rho} A_\nu(p_1) H_{\lambda\rho}(p_2)\sigma(p_1,p_2), \end{aligned} \qquad (5)$$

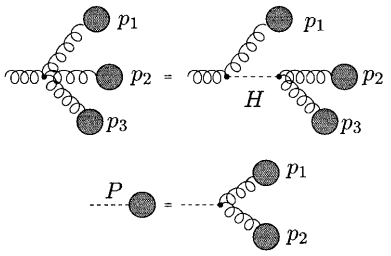

Fig. 5. Elimination of the four-vertex and the new H–gluon–gluon vertex

$$H_{\mu\nu}(P) = -\frac{(g_s)}{4} \sum_{P=p_1+p_2} X^{\mu\nu\lambda\rho} A_\lambda(p_1) A_\rho(p_2)\sigma(p_1,p_2), \qquad (6)$$

where $X^{\mu\nu\lambda\rho}$ is the new H–gluon–gluon vertex:

$$X^{\mu\nu\lambda\rho} = g^{\mu\lambda} g^{\nu\rho} - g^{\nu\lambda} g^{\mu\rho}.$$

These four equations, namely (5), (6), (2) and (3), represent off-shell subamplitudes that are the building blocks of any process. They are used iteratively, combining two (or three) momenta, at each step, to build a subamplitude. The iteration begins with the initial conditions for the external particles. In particular for a gluon we have

$$A^\mu_a(p_i) = \epsilon^\mu_\lambda(p_i)\delta_{aa_i}, \quad i = 1, \ldots, n, \qquad (7)$$

where a is the color, $a = 1, \ldots, 8$, $\epsilon^\mu_\lambda(p)$ denotes the polarization vector and i denotes one the external gluons. For the quarks and antiquarks the iteration starts with

$$\psi_k(p_i) = \begin{cases} u(p_i)\delta_{kk_i} \text{ if } i \text{ incoming}, \\ \bar{u}(p_i)\delta_{kk_i} \text{ if } i \text{ outgoing}, \end{cases}$$

$$\bar{\psi}_k(p_i) = \begin{cases} \bar{u}(p_i)\delta_{kk_i} \text{ if } i \text{ incoming}, \\ u(p_i)\delta_{kk_i} \text{ if } i \text{ outgoing}, \end{cases} \qquad (8)$$

where k is the color, $k = 1, 2, 3$. The next step is combining two of the external momenta, in all possible ways, in accordance to the Feynman rules, to compute the next subamplitude. The iteration goes through in the same manner, using the equations (5), (6), (2) and (3) repeatedly, each time combining the new momenta obtained, with the remaining of the external ones. After $n-1$ steps there is only one momentum left to be combined, so the last step gives us the amplitude $\mathcal{A}(p_1, p_2, \ldots, p_n)$. We refer to [4] for all further details of the algorithm.

2.2 Color and helicity

In order to have an estimate of the production probability, one has to sum over all color and helicity configurations. Summation over colors is a delicate subject. If one performs the summation in a straightforward way then one has to consider something like $8^{n_g} \times 3^{n_q} \times 3^{n_{\bar{q}}}$ configurations for the n-parton scattering, where $n_g, n_q, n_{\bar{q}}$ is the number of gluons, quarks and antiquarks respectively.

In this section we show how this summation can be replaced by integration, which is then suitable for Monte Carlo computation. As a first step a simplification of the color structure is possible by defining the following object [13]:

$$G_{AB} \equiv \sum_{a=1}^{8} t^a_{AB} G^a, \quad A, B = 1, 2, 3, \tag{9}$$

where G^a is the gluon field and all other indices have been temporarily suppressed. The new objects are of course traceless, 3×3 matrices in color space. The interesting property of this color representation is that it leads to a "diagonalization" of the color structure of the three-gluon vertex. More specifically the color part of the three-gluon vertex is now given by

$$f^{abc} t^a_{AB} t^b_{CD} t^c_{EF} = -\frac{\mathrm{i}}{4}(\delta_{AD}\delta_{CF}\delta_{EB} - \delta_{AF}\delta_{CB}\delta_{ED}) \tag{10}$$

(compare Fig.6). This color structure shows the color flow in the real physical process, where gluons can be represented by quark–antiquark states in color space and their self-interaction, as given by (10), reflects the fact that color remains unchanged on an uninterrupted color line. The recursion equations that include the gluon, like (5), now are modified according to (9), to reflect the new color structure. The full content of the recursion equations, including the color structure as just described, is listed in Appendix A.

This new, simplified color structure of the vertices, allows us now to take the next step in making the computation of the color part of an amplitude more efficient, by ridding ourselves of the summations, mentioned in the beginning of this section, and replacing them by integration. To this end, we assign to a fermion a complex vector z_A, where the index runs from 1 to 3, representing its color content. These vectors parameterize the 5-dimensional representation of $SU(3)$ on the sphere and are subjected to the constraint

$$\mid z_1 \mid^2 + \mid z_2 \mid^2 + \mid z_3 \mid^2 = 1.$$

In this space, integration is defined through the proper definition for the invariant group measure, $[\mathrm{d}z]$:

$$\int [\mathrm{d}z] \equiv \int \left(\prod_{i=1}^{3} \mathrm{d}z_i \mathrm{d}z_i^* \right) \delta \left(\sum_{i=1}^{3} z_i z_i^* - 1 \right).$$

We can use a simple polar coordinates parameterization to represent these complex vectors:

$$\begin{aligned} z_1 &= \mathrm{e}^{\mathrm{i}\phi_1} \cos\theta, \\ z_2 &= \mathrm{e}^{\mathrm{i}\phi_2} \sin\theta \cos\xi, \\ z_3 &= \mathrm{e}^{\mathrm{i}\phi_3} \sin\theta \sin\xi, \\ 0 \le \phi_i \le 2\pi; \quad 0 \le \theta \le \frac{\pi}{2}; \quad 0 \le \xi \le \frac{\pi}{2}, \end{aligned} \tag{11}$$

and in terms of these variables, the invariant measure becomes

$$\frac{1}{\pi^3} \left(\prod_{i=1}^{3} \int_0^{2\pi} \mathrm{d}\phi_i \right) \int_0^{\pi/2} \mathrm{d}\theta \int_0^{\pi/2} \mathrm{d}\xi \cos\theta \sin^3\theta \cos\xi \sin\xi.$$

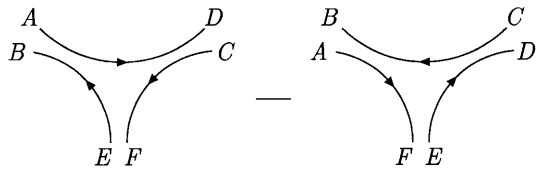

Fig. 6. Color flow in the gluon three-vertex, as represented in (10)

The color structure as described by (10) shows that gluons can be interpreted as quark–antiquark pairs. So we construct the following vector, appropriate for describing the color part of a gluon, which has this color structure:

$$\eta^a(z) = \sqrt{24} \sum_{i,j=1}^{3} z_i^* (t^a)_{ij} z_j, \quad a = 1, \ldots, 8, \tag{12}$$

where t^a are the Gell-Mann matrices. This vector is real, because $(\eta^a)^* = \eta^a$ due to the hermiticity of the Gell-Mann matrices, and is normalized as follows:

$$\int [\mathrm{d}z] \eta^a(z) \eta^b(z) = \delta^{ab}.$$

As far as our recursive equations are concerned: their structure remains unaffected and the only thing to be changed are the initial conditions:

$$\begin{aligned} G^\mu_{AB}(P_i) &= \sum_{a=1}^{8} G^a(P_i) \eta^a(z) \\ &= \sqrt{6} \left(z_{iA} z^*_{iB} - \frac{1}{3} \delta_{AB} \right) \epsilon^\mu_\lambda(P_i), \\ \psi_A(P_i) &= \sqrt{3} u(P_i) z_{iA}, \\ \bar{\psi}_A(P_i) &= \sqrt{3} \bar{u}(P_i) z^*_{iA}, \end{aligned} \tag{13}$$

where as usual $i = 1, \ldots, n$, λ is the helicity and $\vec{z}_i$ are the new continuous color coordinates of the ith parton. The constants in the front are normalizations.

In the same spirit summation over helicity configurations of the external partons can be replaced by an integration over a phase variable. For example, for a gluon this is achieved by introducing the polarization vector

$$\epsilon^\mu_\phi(p) = \mathrm{e}^{\mathrm{i}\phi} \epsilon^\mu(p, +) + \mathrm{e}^{-\mathrm{i}\phi} \epsilon^\mu(p, -),$$

where ϕ is a random number. Then by integrating over ϕ we obtain the sum over helicities,

$$\frac{1}{\pi} \int_0^{\pi} \mathrm{d}\phi \epsilon^\mu_\phi(p) (\epsilon^\nu_\phi(p))^* = \sum_{\lambda=\pm} \epsilon^\mu(p, \lambda) (\epsilon^\nu(p, \lambda))^*.$$

The same thing can be used for the helicity of a quark or an antiquark. For example, for the quark we have

$$u_\phi(p) = \mathrm{e}^{\mathrm{i}\phi} u_+(p) + \mathrm{e}^{-\mathrm{i}\phi} u_-(p),$$

and when integrated over ϕ it gives the sum over polarizations

$$\sum_{\lambda=\pm} u_\lambda(p) \bar{u}_\lambda(p) = \not{p}$$

and the same for an antiquark.

Table 1. The number of distinct processes, as defined in Appendix C, for $f = 5$ final-state flavors, and $f = 4$ initial-state flavors

# of jets	2	3	4	5	6	7	8	9	10
# of dist. processes	10	14	28	36	64	78	130	154	241
total # of processes	126	206	621	861	1862	2326	4342	5142	8641

2.3 The Fermi sign function

Since we are dealing with fermions, we must find a way to incorporate a sign change when we interchange two identical fermions in a process. To this end we use the binary representation of the momentum labels of the external particles (e.g. $P_1 \to (0001), P_2 \to (0010), P_3 = P_1 + P_2 \to (0011)$, etc.) So the sign relative to the permutation of two momenta, $\sigma(P_i, P_j)$ is computed as an operation on the two binary strings representing those momenta, $\sigma(m_i, m_j)$. The function that performs that operation is defined by

$$\sigma(m_1, m_2) = (-1)^{\chi(m_1,m_2)}, \tag{14}$$

with

$$\chi\,(m_1, m_2) = \sum_{i=n}^{2} \hat{m}_{1i} \left(\sum_{j=1}^{i-1} \hat{m}_{2j} \right). \tag{15}$$

A hat over the binary string means that this particular bit is set to 0 if the corresponding external particle is a boson.

2.4 Flavor treatment

The classification of processes contributing to the production of n jets is simplified when certain symmetries are taken into account. For instance processes like $gg \to u\bar{u}u\bar{u}$ and $gg \to d\bar{d}d\bar{d}$ can be grouped together in the general class with representative $gg \to q\bar{q}q\bar{q}$; obviously an extra factor f, representing the number of light flavors, has to be taken into account. We may call the representative "a distinct processes" and attempt a complete classification of such processes. Is clear that the number of distinct processes for a given number n of jets will be a small fraction of the total number of processes; this has a major implication on the computational complexity of the problem, since we may have the total contribution by just computing the contribution of a relatively small number of distinct processes. In Table 1 we give the number of distinct processes, as defined in Appendix C, for $f = 5$ final-state flavors, and $f = 4$ initial-state flavors, where we used these numbers in order to be able to compare with [1].

Another way to tackle all these different processes is to introduce quarks (antiquarks) that are a mixture of different flavors. Thus, keeping with the spirit of color and helicity treatment, we integrate over flavors instead of summing over them. This is done by attaching a vector $\vec{f}$ to each spinor describing a fermion, the components of which are random numbers between 0 and 1:

$$\psi_p = u(p) \times \vec{f},$$

with

$$\vec{f} = \sqrt{N_f} \begin{pmatrix} f_1 \\ f_2 \\ f_3 \\ \vdots \\ f_{N_f} \end{pmatrix},$$

where $f_1, f_2, \ldots, f_{N_f}$ are random numbers and N_f is the number of flavors. We choose the vectors $\vec{f}$ in such a way so that they are normalized as follows:

$$\langle f_i f_j \rangle = \delta_{ij},$$

where $i, j = 1, \ldots, N_f$. As far as the final state is concerned, all flavors are equally treated (massless quarks). In the initial state however, due to different structure functions, special care should be taken of different flavors by a suitable weighting of the initial conditions with the structure function appropriate for each flavor.

In treating flavor as described so far a new "definition" of the concept of distinct process emerges. Any process is now composed by three primary objects, namely g, q and $\bar{q}$, where $q(\bar{q})$ represents a coherent superposition of all flavor states. The possible initial states are nine, namely $gg, gq, g\bar{q}, qg, \bar{q}g, q\bar{q}, \bar{q}q, qq, \bar{q}\bar{q}$ and a final state will be determined by fixing the number m of $q\bar{q}$ pairs. Obviously m should satisfy, $2m \le n - c_i$, with c_i counts the net quark (antiquark) content of the initial state, namely

$$c_{gg} = c_{q\bar{q}} = c_{\bar{q}q} = 0, \quad c_{gq} = c_{qg} = c_{\bar{q}g} = c_{g\bar{q}} = 1,$$
$$c_{qq} = c_{\bar{q}\bar{q}} = 2.$$

So the number of "distinct processes" is now given by

$$9k + 3 \ \text{ if } \ n = 2k \quad \text{and} \quad 9k + 7 \ \text{ if } \ n = 2k + 1, \tag{16}$$

which represents a further reduction compared with the number of distinct processes indicated in the previous table.

3 Jet production rates

The features discussed in the previous sections have been implemented in a FORTRAN code with which we are able to perform perturbative calculations in QCD. We can divide the structure of the calculation leading to jet production rates in four parts: event generation, phase-space generation, squared amplitude computation and sum over processes calculation. In somewhat more detail these parts consist of the following.

Amplitude computation

The basic structure of the algorithm for the amplitude was discussed in Sect. 2. In order to obtain squared amplitudes we use projection to a continuous color space and color MC integration and integration over helicity states. What remains to be done is the ability to extract information about the color string of the final states so that it can be used in codes like HERWIG [10]. Work is being done towards this end [18].

Phase-space generation

In the current status of the code we have implemented two ways of phase-space generation. First of all we have RAMBO [8], a flat phase-space generator which has been around for many years and has proved reliable for the relevant calculations. Recently though, a new generator has been developed, SARGE [11], which take into account the so-called antenna structure of QCD amplitudes. So far it has been proved very efficient for the generation of this type of phase space [9].

Event generation

Let us consider the scattering of two hadrons. The content of a hadron is characterized by the parton structure function $f(x, Q^2)$ where x is the fraction of the momentum P of the hadron, carried by the parton, $p = xP$, and Q^2 is the QCD scale. The cross section for the scattering of two hadrons is given by the sum of all subprocesses between the parton constituents of the hadrons, weighted with the corresponding structure functions of the incoming partons:

$$\sigma(s) = \sum_{ij\,P} \int_0^1 \mathrm{d}x_1 \mathrm{d}x_2 \int \mathrm{d}\Phi F_i(x_1) F_j(x_2) \left(\frac{\mathrm{d}\hat{\sigma}}{\mathrm{d}\Phi}\right)_{ij}, \quad (17)$$

where s is the center of mass (CM) energy squared at the hadron level. As usual the functions $F_m(x)$ are defined by $F_m(x) = f_m(x)/x$, where $f_m(x)$ are the various parton structure functions. The quantities $(\mathrm{d}\hat{\sigma}/\mathrm{d}\Phi)_{ij}$ are the matrix element squared, summed (i.e. integrated) over helicity and color degrees of freedom, and $\mathrm{d}\Phi$ is the element of the phase space. The sum (i.e. integral) is over all partonic processes. We use (17) to estimate jet production rates.

Sum over processes

Finally, once given the number of jets, we are able to compute all the relevant subprocesses that contribute at one go. This is done by randomly choosing a subprocess and then using Monte Carlo to obtain the total cross section from all contributions. The random choice of a subprocess is based on the choice of a pair of integers (i, m), i selecting one out of the nine possible initial states, and m being the number of $q\bar{q}$ pairs in the final state, see (16).

There is also the option to use an optimization based on the fact that some processes overwhelm the total cross section over others (for example the purely gluonic process, $gg \to ng$ has the largest cross section by an order of magnitude, compared to processes with different initial or final states).

The algorithm has been used firstly to compute cross sections for 4 and 5 jet production. We have chosen a CM energy of $s^{1/2} = 14\,\mathrm{TeV}$ and we apply the following cuts:

$$p_{\mathrm{T}i} > 60\,\mathrm{GeV}, \quad \theta_{ij} > 30^\circ, \quad |\eta_i| < 3,$$

where $p_{\mathrm{T}} = (p_x^2 + p_y^2)^{1/2}$ is the transverse momentum of a jet, $\theta_{ij} = (\vec{p}_i, \vec{p}_j)$, is the angle between jets and $\eta = -\ln\tan(\theta/2)$, is the pseudo-rapidity.

For convenience all results are obtained with a non-running strong coupling constant put equal to unity. There are several parameterizations for the parton structure functions in the literature. The one that we will use is the MRST parameterization [15], and the number of light flavors is taken to be $f = 5$.

In Table 2 we have listed several subprocesses and their cross sections, relative for pp scattering at LHC. The table is organized as follows: we are not referring to a particular quark flavor, so we use the letters q, r, s to denote quarks or antiquarks. Since we consider all quarks and antiquarks massless it makes no difference which particular flavor appears in the final state. We compare our results with those from a well established code, NJETS. We also show distributions of the maximum p_{T} for two processes, namely $gg \to gggg$ and $q\bar{q} \to r\bar{r}s\bar{s}$.

To show the potential of the flavor integration method we calculate the total cross section for a set of possible final states and compare with NJETS where as usual a sum over different flavor states has been used. The results are presented in Table 3. We have used the letter q to denote any flavor and all combinations have been taken into account in the calculation of the cross section. We have used the same cuts and CM energy as before.

We have also obtained the total cross sections for the production of 3, 4, 5, 6, 7 and 8 jets. These are listed in Table 4. Also shown there is the contribution of the purely gluonic process to the total cross section. We see the fraction of this process compared to the total is diminishing with increasing number of jets, as was already commented in [16].

Finally we have plotted distributions of the total cross section for the production of 5, 6 and 7 jets. The quantities shown are

(1) the transverse momenta p_{T} of the products, and
(2) the invariant masses $M_{ij} = (2(p_i \cdot p_j))^{1/2}$.

4 Summary

We have presented a procedure to calculate matrix elements and cross sections in QCD using an iterative algorithm based on the Schwinger–Dyson equation. Thus we free ourselves from the task of computing all Feynman graphs for a process, a task which can become impossible even for a moderate number of particles involved.

Table 2. Production rates for 4 and 5 jet production. All results have an estimated error of 4%

Process	$\sqrt{s} = 14\,\text{TeV}$ *OUR CODE* (nb)	*NJETS* (nb)
$gg \to gggg$	2.681	2.533
$q\bar{q} \to gggg$	0.0020	0.0021
$qg \to qggg$	1.131	1.159
$gg \to q\bar{q}gg$	0.106	0.104
$q\bar{q} \to q\bar{q}gg$	0.062	0.059
$q\bar{q} \to r\bar{r}gg$	0.586×10^{-3}	0.558×10^{-3}
$qq \to qqgg$	0.134	0.126
$q\bar{r} \to q\bar{r}gg$	0.171	0.161
$qr \to qrgg$	0.210	0.197
$qg \to q\bar{q}qg$	0.035	0.033
$qg \to r\bar{r}qg$	0.032	0.035
$gg \to q\bar{q}q\bar{q}$	0.524×10^{-3}	0.526×10^{-3}
$gg \to q\bar{q}r\bar{r}$	1.059×10^{-3}	1.074×10^{-3}
$q\bar{q} \to q\bar{q}q\bar{q}$	0.807×10^{-3}	0.851×10^{-3}
$q\bar{q} \to q\bar{q}r\bar{r}$	0.866×10^{-3}	0.786×10^{-3}
$q\bar{q} \to r\bar{r}r\bar{r}$	7.94×10^{-6}	7.93×10^{-6}
$q\bar{q} \to r\bar{r}s\bar{s}$	1.54×10^{-5}	1.49×10^{-5}
$qq \to qqq\bar{q}$	1.64×10^{-3}	1.60×10^{-3}
$qq \to qqr\bar{r}$	1.67×10^{-3}	1.60×10^{-3}
$qr \to qrq\bar{q}$	2.78×10^{-3}	2.91×10^{-3}
$qr \to qrs\bar{s}$	2.63×10^{-3}	2.57×10^{-3}
$q\bar{r} \to q\bar{r}q\bar{q}$	2.28×10^{-3}	2.41×10^{-3}
$q\bar{r} \to q\bar{r}r\bar{r}$	2.20×10^{-3}	2.07×10^{-3}
$q\bar{r} \to q\bar{r}s\bar{s}$	2.39×10^{-3}	2.12×10^{-3}

Process	$\sqrt{s} = 14\,\text{TeV}$ *OUR CODE*(pb)	*NJETS*(pb)
$gg \to ggggg$	159.49	160.40
$q\bar{q} \to ggggg$	0.141	0.136
$qg \to qgggg$	87.94	84.37
$gg \to q\bar{q}ggg$	9.193	9.218
$q\bar{q} \to q\bar{q}ggg$	4.37	4.561
$q\bar{q} \to r\bar{r}ggg$	0.034	0.0348
$qq \to qqggg$	11.47	12.35
$q\bar{r} \to q\bar{r}ggg$	11.39	11.98
$qr \to qrggg$	16.51	17.29
$qg \to q\bar{q}qgg$	3.858	3.799
$qg \to r\bar{r}qgg$	3.738	3.887
$gg \to q\bar{q}q\bar{q}g$	0.104	0.101
$gg \to q\bar{q}r\bar{r}g$	0.207	0.206
$q\bar{q} \to q\bar{q}q\bar{q}g$	0.252	0.259
$q\bar{q} \to q\bar{q}r\bar{r}g$	0.230	0.254
$q\bar{q} \to r\bar{r}r\bar{r}g$	0.0020	0.0020
$q\bar{q} \to r\bar{r}s\bar{s}g$	0.0038	0.0038
$qq \to qqq\bar{q}g$	0.684	0.691
$qq \to qqr\bar{r}g$	0.698	0.659
$qr \to qrq\bar{q}g$	0.998	0.922
$qr \to qrs\bar{s}g$	0.862	0.941
$q\bar{r} \to q\bar{r}q\bar{q}g$	0.684	0.658
$q\bar{r} \to q\bar{r}r\bar{r}g$	0.650	0.678
$q\bar{r} \to q\bar{r}s\bar{s}g$	0.634	0.665
$qg \to q\bar{q}q\bar{q}q$	0.0352	0.0334
$qg \to q\bar{q}r\bar{r}q$	0.0646	0.0682
$qg \to r\bar{r}r\bar{r}q$	0.0328	0.0328
$qg \to r\bar{r}s\bar{s}q$	0.0650	0.0668

Table 3. Flavor integration with an estimated error of 2%

Process	$\sqrt{s} = 14\text{TeV}$ *OUR CODE* (nb)	*NJETS* (nb)
$q\bar{q} \to q\bar{q}gg$	0.242	0.232
$q\bar{q} \to q\bar{q}q\bar{q}$	0.015	0.014
$qq \to qqgg$	0.311	0.322
$gg \to q\bar{q}q\bar{q}$	0.013	0.014
$qg \to q\bar{q}qg$	0.167	0.174

We have also managed to bypass the computationally expensive procedure of summing over all possible color and helicity configurations, by introducing continuous vectors to represent these otherwise discrete quantities and using Monte Carlo integration instead of summation. At this stage our code can reliably compute scattering amplitudes and cross sections

(1) for individual, single-flavor processes;
(2) for processes where a sum over all contributing flavors is needed both in the initial or the final states;
(3) for total jet cross sections, where we are interested in production rates with a contribution from all possible subprocesses and all flavors.

Our future interests involve a convolution of this code with fragmentation codes like HERWIG, so that one can perform realistic simulations of multi-jet processes.

Appendix

A The complete recursion relations

Below we give the full recursion equations including the color.

(1) Gluon field $A^\mu(p)$:

$$
\begin{aligned}
A^\mu_{AB}(P) = {} & \frac{g_s}{2P^2} \sum_{P=p_1+p_2} \Bigg\{ \bar{\psi}_B(p_1)\gamma^\mu\psi_A(p_2) \\
& - \frac{1}{3}\left(\sum_C \bar{\psi}_C(p_1)\gamma^\mu\psi_C(p_2)\right)\delta_{AB}\Bigg\}\sigma(p_1,p_2) \\
& + \frac{g_s}{2P^2} \sum_{P=p_1+p_2} V^{\mu\nu}_\lambda(P,p_1,p_2)\Big\{A^\nu_{AC}(p_1)A^\lambda_{CB}(p_2) \\
& - A^\lambda_{AC}(p_2)A^\nu_{CB}(p_1)\Big\}\sigma(p_1,p_2) \\
& + \frac{\mathrm{i}g_s}{2P^2} \sum_{P=p_1+p_2} X^{\mu\nu}_{\lambda\rho}\Big\{A^\nu_{AC}(p_1)H^{\lambda\rho}_{CB}(p_2) \\
& - H^{\lambda\rho}_{AC}(p_2)A^\nu_{CB}(p_1)\Big\}\sigma(p_1,p_2).
\end{aligned}
$$

(2) Auxiliary field $H_{\mu\nu}(p)$:

$$
\begin{aligned}
H^{\mu\nu}_{AB}(P) = {} & \frac{(\mathrm{i}g_s)}{4} \sum_{P=p_1+p_2} X^{\mu\nu}_{\lambda\rho}\{A^\lambda_{AC}(p_1)A^\rho_{CB}(p_2) \\
& - A^\rho_{AC}(p_2)A^\lambda_{CB}(p_1)\}\sigma(p_1,p_2).
\end{aligned}
$$

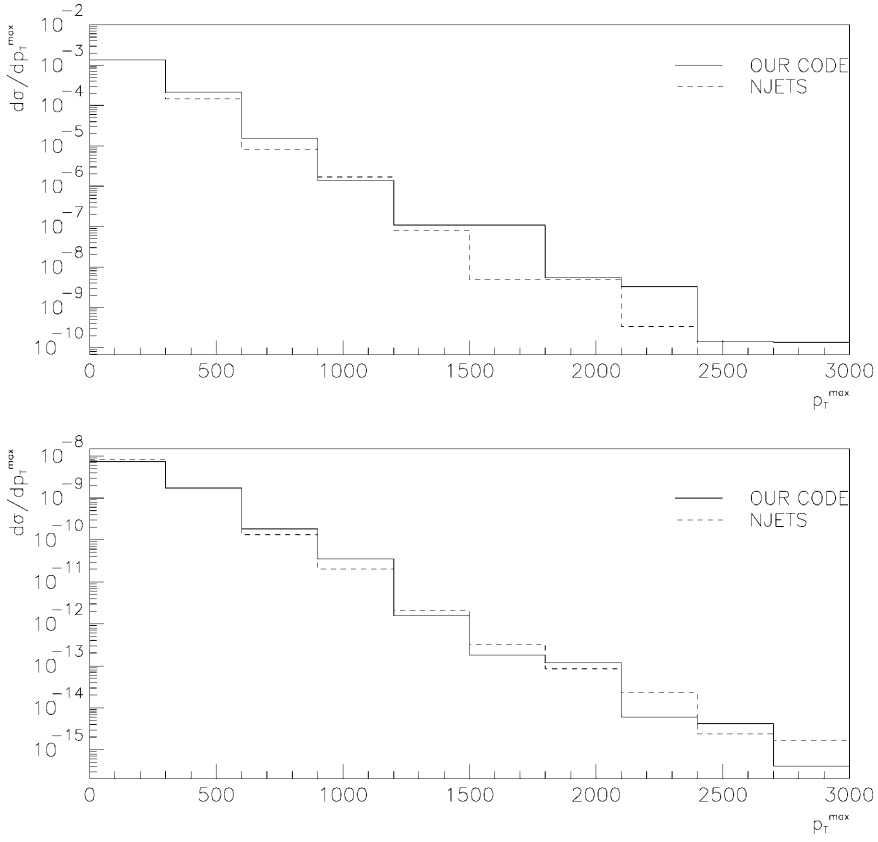

Fig. 7. Maximum $p_{\rm T}$ distributions for $gg \to gggg$ (top plot) and $q\bar{q} \to r\bar{r}s\bar{s}$ (bottom plot)

Table 4. Total cross sections for the production of up to 8 jets. The last row shows the percentage contribution of the purely gluonic process ($gg \to ng$). The estimated error is 3% for 3 and 4 jets, 4% for 5 and 6 jets and 6% for 7 and 8 jets

# of jets	3	4	5	6	7	8
$\sigma(nb)$	91.41	6.54	0.458	2.97×10^{-2}	2.21×10^{-3}	2.12×10^{-4}
% Gluonic	45.7	39.2	35.7	35.1	33.8	26.6

(3) Fermion field $\psi_A(p)$:

$$\psi_A(P) = \frac{g_s}{P^2} \sum_{P=p_1+p_2} \not{P} \not{A}_{AB}(p_1)\psi_B(p_2)\sigma(p_1,p_2).$$

(4) Antifermion field $\bar{\psi}_A(p)$:

$$\bar{\psi}_A(P) = \frac{g_s}{P^2} \sum_{P=p_1+p_2} \bar{\psi}_B(p_2) \not{A}_{BA}(p_1) \not{P} \sigma(p_1,p_2).$$

B Counting diagrams

In this appendix we show how the number of tree-level graphs for a general QCD process can be determined. This is done in the same recursive manner as that in which the amplitudes are computed. Let there be k quark flavors. We shall compute the number of graphs that take a single specified parton into a number of specified partons, as follows. Let us denote by $a_i(n_0, n1, \bar{n}_1, n_2, \bar{n}_2, \ldots, n_k, \bar{n}_k)$ the number of graphs with a quark of type i coming in and ending up in n_0 gluons, n_1 quarks of type 1, $\bar{n}_1$ antiquarks of type 1, and so on. We define the following generating function:

$$\psi(z, x_1, \bar{x}_1, x_2, \bar{x}_2, \ldots, x_k, \bar{x}_k) = \sum_{n_0,n_1,\ldots,\bar{n}_k \geq 0} a_i(n_0, n_1, \bar{n}_1, n_2, \bar{n}_2, \ldots, n_k, \bar{n}_k) \times \frac{z^{n_0} x_1^{n_1} \bar{x}_1^{\bar{n}_1} x_2^{n_2} \cdots \bar{x}_k^{\bar{n}_k}}{n_0! n_1! \bar{n}_1! n2! \cdots \bar{n}_k!}.$$

The generating functions $\bar{\psi}$ for incoming antiquarks, and ϕ for incoming gluons, are defined in an analogous manner. The Feynman rules of QCD then tell us that the various generating functions are related in the following manner:

$$\psi_i = x_i + \psi_i \phi,$$
$$\bar{\psi}_i = \bar{x}_i + \bar{\psi}_i \phi,$$
$$\phi = z + \frac{1}{2}\phi^2 + \frac{1}{6}\phi^3 + \sum_{i=1}^{k} \psi_i \bar{\psi}_i.$$

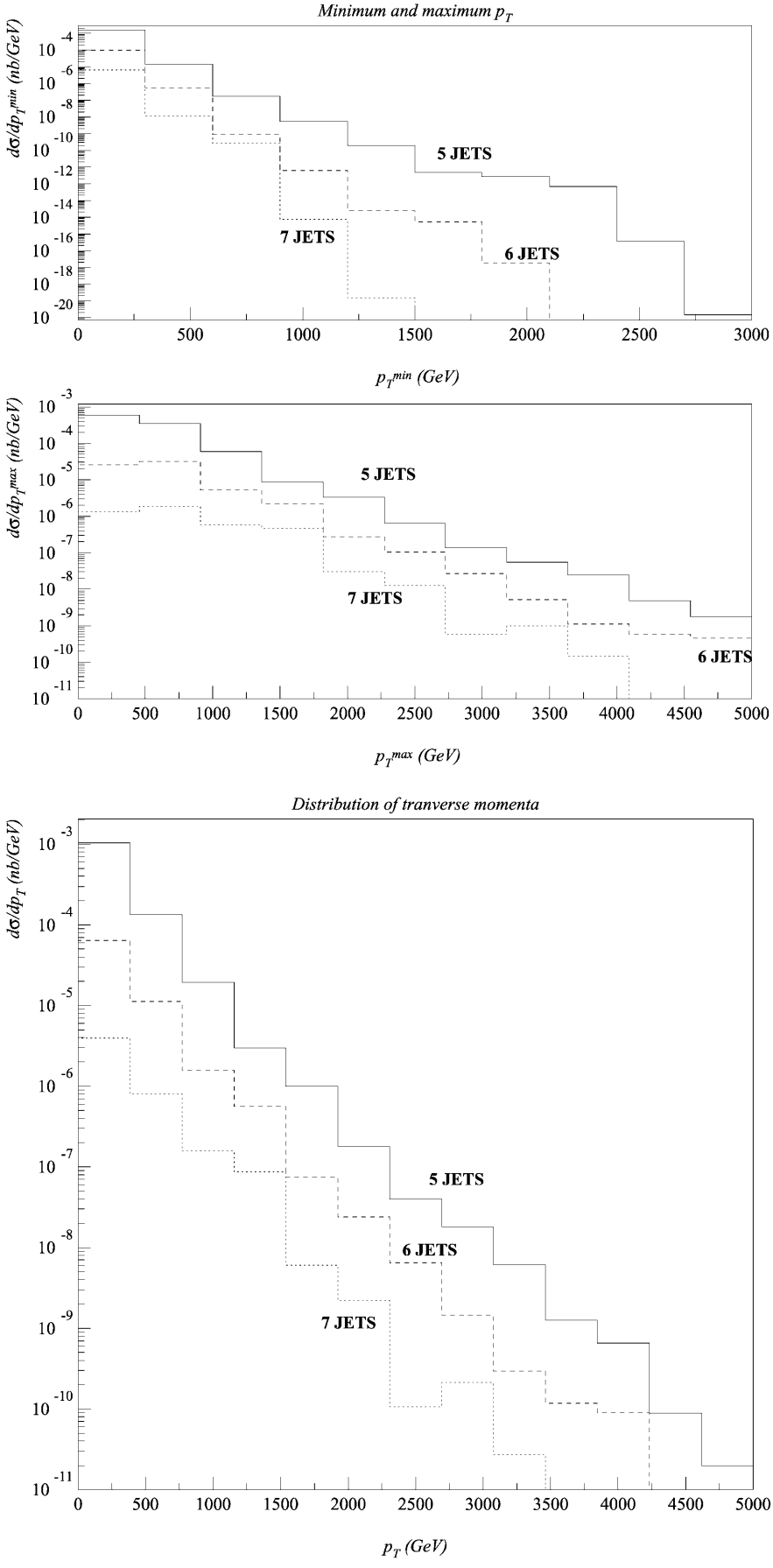

Fig. 8. p_{T} distributions for 5, 6 and 7 jet production

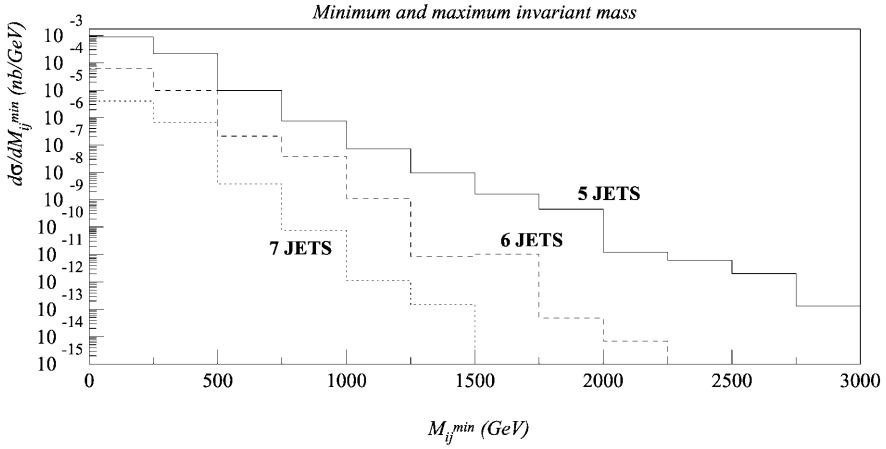

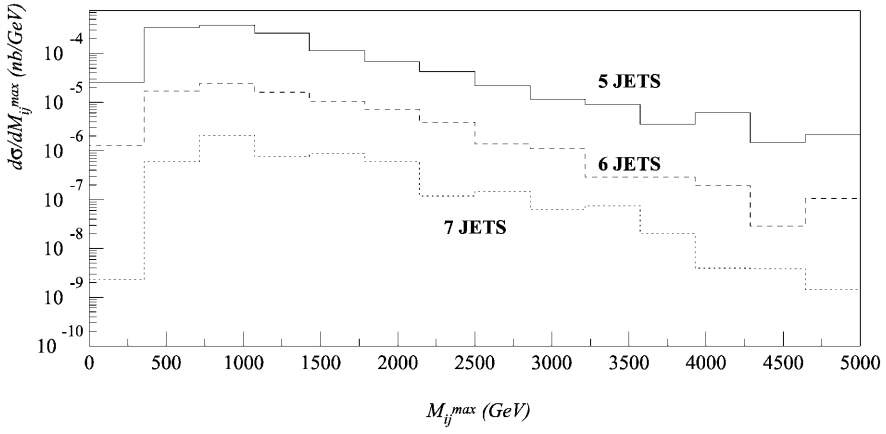

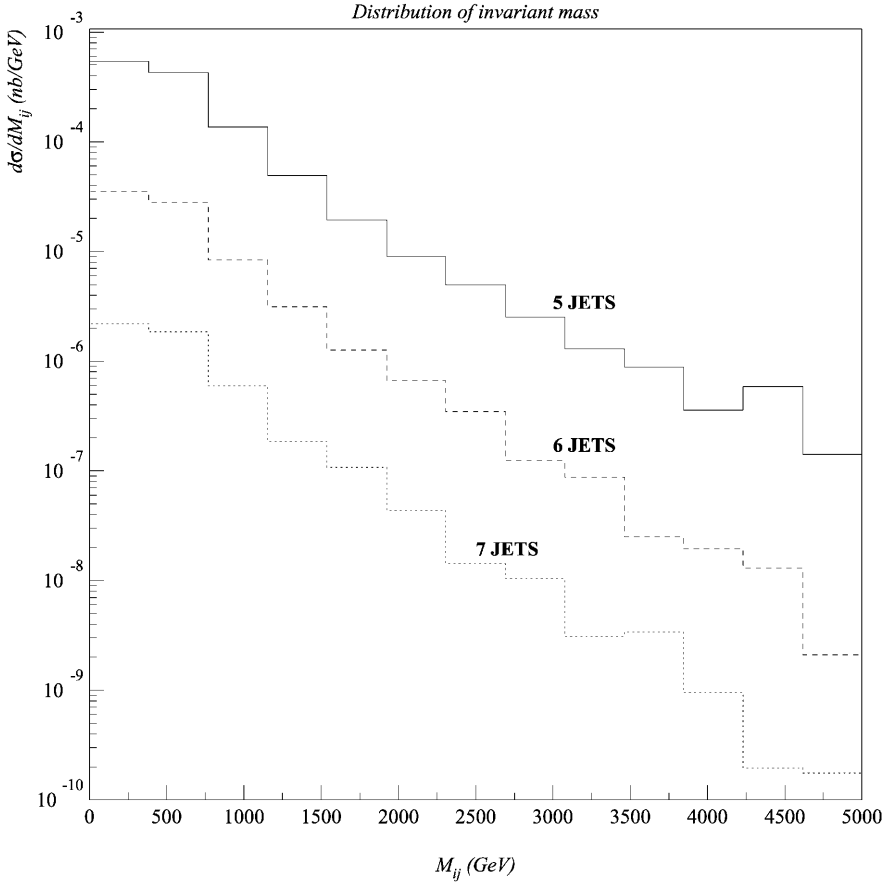

Fig. 9. Invariant mass distributions for 5, 6 and 7 jet production

Table 5. The five types of initial states (not counting trivial charge conjugation), with the corresponding number of distinct processes, and the functions needed to compute their multiplicity factors

Initial-state type		Distinct processes	Multiplicity factor
A	(gg)	$C_1(n)$	$\chi(n_0, n_1, \ldots, n_f; f)$
B	$(q\bar{q})$	$C_2(n)$	$\chi(n_0, n_2, \ldots, n_f; f-1)$
C	$(gq$ and $qg)$	$C_2(n-1)$	$\chi(n_0, n_2, \ldots, n_f; f-1)$
D	(qq)	$C_2(n-2)$	$\chi(n_0, n_2, \ldots, n_f; f-1)$
E	$(qq'$ and $q\bar{q}')$	$C_3(n-2)$	$\chi(n_0, n_3, \ldots, n_f; f-2)$

These can trivially be solved in such a way that everything is expressed in terms of ϕ:

$$\psi_i = x_i/(1-\phi), \quad \bar{\psi}_i = \bar{x}_i/(1-\phi),$$

and

$$\phi = z + \frac{1}{2}\phi^2 + \frac{1}{6}\phi^3 + \frac{\xi}{(1-\phi)^2}, \quad \xi = \sum_{i=1}^{k} x_i \bar{x}_i.$$

The number of different quark flavors is seen not to be a complication here. By computer algebra, the function ϕ can easily be obtained to quite high order in z and the x's, and the number of diagrams read off from the corresponding coefficient. A similar discussion can be found in [7], but we feel that the above procedure is simpler and moreover leads itself to estimates of the asymptotic number of graphs for very large multiplicities [17].

C Counting distinct processes

We start by tabulating in Table 5 the five types of initial states (not counting trivial charge conjugation), with the corresponding number of distinct processes, and the functions needed to compute their multiplicity factors. We denote by n the number of final-state partons.

In order to clarify what we mean we consider the example of the type A initial state. Each distinct process is defined by an array $(n_0, n_1, \ldots, n_f)$. For instance, in the case of four-jet production we have

$$\begin{aligned}
&(4,0,0,0,0,0) \quad gg \to gggg,\\
&(2,1,0,0,0,0) \quad gg \to ggq\bar{q},\\
&(0,2,0,0,0,0) \quad gg \to q\bar{q}q\bar{q},\\
&(0,1,1,0,0,0) \quad gg \to q\bar{q}r\bar{r}.
\end{aligned}$$

Therefore, in order to count the distinct processes we need the following three functions:

$$C_1(n) = \sum_{n_0+2n_1+\ldots+2n_f=n} \Theta(n_1 \geq n_2 \geq \ldots \geq n_f),$$

$$C_2(n) = \sum_{n_0+2n_1+\ldots+2n_f=n} \Theta(n_2 \geq n_3 \geq \ldots \geq n_f),$$

and

$$C_3(n) = \sum_{n_0+2n_1+\ldots+2n_f=n} \Theta(n_3 \geq n_4 \geq \ldots \geq n_f).$$

Of course each distinct process, given by the array $(n_0, n_1, \ldots, n_f)$ has a multiplicity factor that is easily computed:

$$\chi(n_0, n_1, \ldots, n_f; f) = n_f(n_f-1)\ldots(n_f-j+1)/j!,$$

where j is defined by

$$\begin{aligned}
j = f \quad &\text{if} \quad \prod_{i=1}^{f} n_i \neq 0,\\
j = f-1 \quad &\text{if} \quad \prod_{i=1}^{f-1} n_i \neq 0,\\
&\ldots\\
j = 1 \quad &\text{if} \quad n_1 \neq 0,\\
j = 0 \ &\text{otherwise.}
\end{aligned}$$

Results for $f = 5$ final-state flavors and $f = 4$ initial-state flavors are shown in Table 1 of Sect. 2, in the discussion of flavor treatment, just to compare with [1].

Moreover it is very easy to produce the list of the distinct processes to be computed for each case as well as the multiplicity factors χ. A code doing this is available.

To study high-n behavior we may use the generating function technique. Then we get

$$F_1(x) = \sum_{n=0}^{\infty} C_1(n)x^n = \frac{1}{(1-x)} \prod_{j=1}^{f} \frac{1}{(1-x^{2j})},$$

$$F_2(x) = \sum_{n=0}^{\infty} C_2(n)x^n = \frac{1}{(1-x)(1-x^2)} \prod_{j=1}^{f-1} \frac{1}{(1-x^{2j})},$$

$$F_3(x) = \sum_{n=0}^{\infty} C_3(n)x^n = \frac{1}{(1-x)(1-x^2)^2} \prod_{j=1}^{f-2} \frac{1}{(1-x^{2j})}.$$

As one can easily see, the order of the pole at $x = 1$ is always given by $f + 1$.

Our results may be compared directly to those obtained in [1]. In fact, using our method, we were able to detect several errors in Table 9.3, page 125, among which the fact that a processes is missing for the cases $m = 6$ and $m = 7$, namely $qr \to qrr\bar{r}(g)$. Correcting for this error we get full agreement.

References

1. J.G.M. Kuijf, Multiparton production at hadron colliders, PhD thesis (University of Leiden) (1991)
2. W.T. Giele, Properties and calculations of multiparton processes, PhD thesis (University of Leiden) (1989)
3. F. Caravaglios, M. Moretti, Phys. Lett. B **358**, 332 (1995)
4. A. Kanaki, C.G. Papadopoulos, Comput. Phys. Commun. **132**, 306 (2000)

5. F.A. Berends, C.G. Papadopoulos, R. Pittau, hep-ph/0002249
6. M.A.B. Beg, H. Ruegg, J. Math. Phys. **6**, 677 (1965)
7. F. Caravaglios, M.L. Mangano, M. Moretti, R. Pittau, Nucl. Phys. B **539**, 215 (1999)
8. W.J. Stirling, R. Kleiss, S.D. Ellis, Comp. Phys. Comm. **40**, 359 (1986)
9. A. van Hameren, R. Kleiss, P.D. Draggiotis, Phys. Lett. B **483**, 124 (2000)
10. G. Corsella, et al., JHEP **0101**, 010 (2001)
11. A. van Hameren, R. Kleiss, Eur. Phys. J. C **17**, 611 (2000); hep-ph/0008068
12. A. van Hameren, Loaded dice in Monte-Carlo, PhD thesis (University of Nijmegen) (2001)
13. P.D. Draggiotis, R. Kleiss, C.G. Papadopoulos, Phys. Lett. B **439**, 157 (1998)
14. Z. Kunszt, W.J. Stirling, in Proceedings Workshop on Physics at Future Accelerators, edited by J.H. Mulvey, CERN 87-07, vol. 2, La Thuile and Geneva, p. 548; Phys. Rev. D **37**, 2439 (1988)
15. A.D. Martin, R.G. Roberts, W.J. Stirling, R.S. Thorne, Eur. Phys. J. C **14**, 133 (2000)
16. P.D. Draggiotis, R. Kleiss, Eur. Phys. J. C **17**, 437 (2000); hep-ph/0006133
17. R. Kleiss, P.D. Draggiotis, hep-ph/0110225
18. R. Kleiss, C.G. Papadopoulos, P.D. Draggiotis, in preparation